ACS APPLIED MATERIALS & INTERFACES

RESEARCH ARTICLE

www.acsami.org

Synthesis and Electromagnetic, Microwave Absorbing Properties of Core−Shell Fe_3O_4−Poly(3, 4-ethylenedioxythiophene) Microspheres

Wencai Zhou,[†,‡] Xiujie Hu,[*,†] Xiaoxia Bai,[†,‡] Shuyun Zhou,[*,†] Chenghua Sun,[†] Jun Yan,[†] and Ping Chen[†]

[†]Key Laboratory of Photochemical Conversion and Optoelectronic Materials, Technical Institute of Physics and Chemistry, Chinese Academy of Sciences, Beijing 100190, China

[‡]Graduate University of Chinese Academy of Sciences, Beijing 100049, China

ABSTRACT:

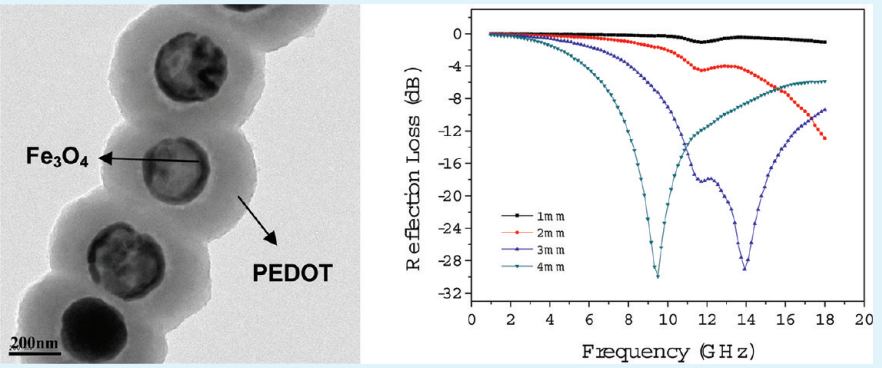

Highly regulated core−shell Fe_3O_4−poly(3, 4-ethylenedioxythiophene) (PEDOT) microspheres were successfully synthesized by a two-step method in the presence of polyvinyl alcohol (PVA) and *p*-toluenesulfonic acid (*p*-TSA). And their morphology, microstructure, electromagnetic and microwave absorbing properties were subsequently characterized. By simply adjusting the molar ratio of 3, 4-ethylenedioxythiophene (EDOT) to Fe_3O_4 (represented by (EDOT)/(Fe_3O_4)), the thickness of the polymer shell can be tuned from tens to hundreds of nanometers. Moreover, it was found that the composite exhibited excellent microwave absorbing property with a minimum reflection loss (RL) of about −30 dB at 9.5 GHz with a (EDOT)/(Fe_3O_4) ratio of 20.

KEYWORDS: Fe_3O_4−PEDOT composite, core−shell, electromagnetic, two-step method, microwave absorbing, reflection loss

INTRODUCTION

Recently, the conjugation of conducting polymers and inorganic magnetic nanoparticles has attracted more attention because the resultant materials not only exhibit a combination of the conductive and magnetic properties but also take the advantages of both nanomaterials and polymers. Besides, the inorganic magnetic nanoparticles coated by the conducting polymers will be prevented from reuniting caused by high surface activity. Therefore, these conductive and magnetic composites have great potential applications in the fields of electrical and magnetic shields, molecular electronics, nonlinear optics and microwave absorbing materials.[1−4]

Among magnetic metal oxides, Fe_3O_4 with properties of superparamagnetism in addition to its low toxicity and high biocompatibility is the most-studied material for magnetic nanoparticles[5] in magnetic storagemedia, contrast agents for magnetic resonance imaging (MRI),[6] separation of biomolecules,[7] environmental or food analyzes,[8] immunoassays,[9] controlling targeted drug delivery/release,[10] and microwave absorbing.[11]

Up to now, the researches on the fabrication of conductive and magnetic composites base on Fe_3O_4 are mainly focused on Fe_3O_4−polypyrrole/polyaniline (Fe_3O_4−PPy/PANI). Liu et al. synthesized electric and ferromagnetic Fe_3O_4−PPy composites by a chemical method using *p*-dodecylbenzene sulfonic acid sodium salt (NaDS) as surfactant and dopant.[12] Deng et al. prepared core−shell Fe_3O_4−PPy nanoparticles and demonstrated that both the conductivity and the magnetization of the composites strongly depended on the Fe_3O_4 content and the doping degree.[13] Lu et al. also synthesized highly regulated core−shell Fe_3O_4−PPy microspheres with low conductivity.[14] On the other hand, Reddy et al. synthesized electromagnetic functionalized Fe_3O_4−PANI composites with ammonium peroxydisulfate as the oxidizing agent.[15]

Poly (3,4-ethylenedioxythiophene) (PEDOT), a polythiophene derivative, is one of the most promising conductive polymers with excellent electrochemical activity, high electrical conductivity, moderate band gap, low redox potential, and excellent environmental stability. And in our recent study, we have revealed the microwave absorbing ability of PEDOT.[16] Therefore, the composite consisted of Fe_3O_4 and PEDOT will have an attractive prospect. Reddy et al. have synthesized core−shell nanocomposite composed of Fe_3O_4 nanoparticles and

Received: April 18, 2011
Accepted: September 13, 2011
Published: September 13, 2011

PEDOT with lignosulfonic acid (LSA) serving as both the surfactant and the dopant.[17] Even so, the preparation of highly regulated core−shell Fe_3O_4−PEDOT micro- or nanospheres is still a challenge, which was rarely reported.

Here, we propose a two-step method for the preparation of Fe_3O_4 microspheres with an integrated PEDOT shell. Fe_3O_4 hollow microspheres were first synthesized by solvothermal method,[18] which has the advantage of lightweight in microwave absorbing, followed by EDOT polymerization on the microsphere surface. By simply adjusting the molar ratio of 3, 4-ethylenedioxythiophene (EDOT) to Fe_3O_4 (represented by (EDOT)/(Fe_3O_4)), the shell thickness of the composite, hence the electrical and magnetic properties, could be tuned. During the formation, polyvinyl alcohol (PVA) was used as stabilizer while *p*-toluenesulfonic acid (*p*-TSA) served as the dopant. The obtained composites exhibited excellent microwave absorbing property at appropriate shell thickness, with the maximum microwave absorbing reached about −30 dB at 9.5 GHz.

EXPERIMENTAL SECTION

All reagents were used directly as received unless otherwise mentioned.

Synthesis of Hollow Fe_3O_4 Microspheres. Fe_3O_4 hollow microspheres were synthesized according to literature:[18] $FeCl_3 \cdot 6H_2O$ (2 mmol) and urea (6 mmol) were first dissolved in absolute ethylene glycol (25 mL). Then the solution was loaded into a Teflon-lined stainless steel autoclave. The autoclave was sealed and maintained at 200 °C for a definite time. After cooling to room temperature naturally, the black products were filtered off, washed with distilled water and absolute ethanol several times, and dried under a vacuum at 60 °C for 20 h.

Synthesis of Fe_3O_4−PEDOT Composites. The as-prepared hollow Fe_3O_4 microspheres were immersed in PVA (0.4 g) aqueous solution with ultrasonic for 20 min. *p*-TSA (20 mmol) was then added to the above mixture. The mixture was stirred for 20 min, and then EDOT (1 mmol) was introduced with stirring for 24 h. At last, ammonium persulfate (APS) (1 mmol) was added to prepare 100 mL of the mixture. After being stirred for 24 h at room temperature, the mixture was centrifuged and washed three times with a solvent of deionized water/ethanol (1/1, v/v). The precipitate was dried under a vacuum at 60 °C for 24 h.

Measurements. The morphology of the products was investigated using JEM-2100F transmission electron microscope (TEM). Fourier transform infrared (FTIR) spectra in the range of 500−2000 cm^{-1} were conducted on sample pellets with KBr by means of an infrared spectrophotometer (Excalibur 3100, America, Varian).The phase identification of the fine powder composite was performed using X-ray diffraction (XRD) analysis on a D8 Focus Diffractometer (Germany). Conductivity measurements of the Fe_3O_4−PEDOT samples (compressed into rectangular block) were performed using a Keithley 220 Source Meter four-point probe instrument. Magnetic properties were tested by vibrating sample magnetometer (VSM, Lakeshore 707 Series). The composites samples for electromagnetic parameter measurement were prepared by mixing the Fe_3O_4−PEDOT microspheres and paraffin wax at different volume fraction of the Fe_3O_4−PEDOT microspheres. The mixture was then pressed into a toroidal shape with the thickness of 2 mm. Subsequently, the relative complex permeability (μ_r) and permittivity (ε_r) were carried out by a HP8722ES network analyzer at the frequency range of 2−18 GHz and the reflection losses were calculated using the measured μ_r and ε_r.

RESULTS AND DISCUSSION

Characterizations. Figure 1a shows the morphology of Fe_3O_4 hollow microspheres. The particles are spherical with diameters ranging from 200−400 nm and a wall thickness of about 50 nm. The density of the prepared Fe_3O_4 microspheres is 3.56 g cm^{-3} because of the existence of a hollow cavity, which is lower than that of the bulk Fe_3O_4. Figure 1b−f shows the morphology of the obtained Fe_3O_4−PEDOT core−shell microspheres prepared with different (EDOT)/(Fe_3O_4) ratios. It is clear that the Fe_3O_4 microspheres are fully coated by PEDOT and the shell gradually thickens with the increase of the (EDOT)/(Fe_3O_4) ratio. When (EDOT)/(Fe_3O_4) ratio is 10, the shell thickness is about 60 nm (Figure 1b). The shells increase to about 90 and 140 nm when (EDOT)/(Fe_3O_4) ratios are at 15 (Figure 1c) and 20 (Figure 1d), respectively. When (EDOT)/(Fe_3O_4) ratio reaches 30, the shell thickness can reach 250 nm (Figure 1e). Further, the shell thickness increases little when the (EDOT)/(Fe_3O_4) ratio continues to increase to 50 (Figure 1f). There will be a saturation shell thickness if the (EDOT)/(Fe_3O_4) ratio continuously increases. The above results indicate that the (EDOT)/(Fe_3O_4) ratio has a significant influence on the structure of the Fe_3O_4−PEDOT core−shell microspheres.

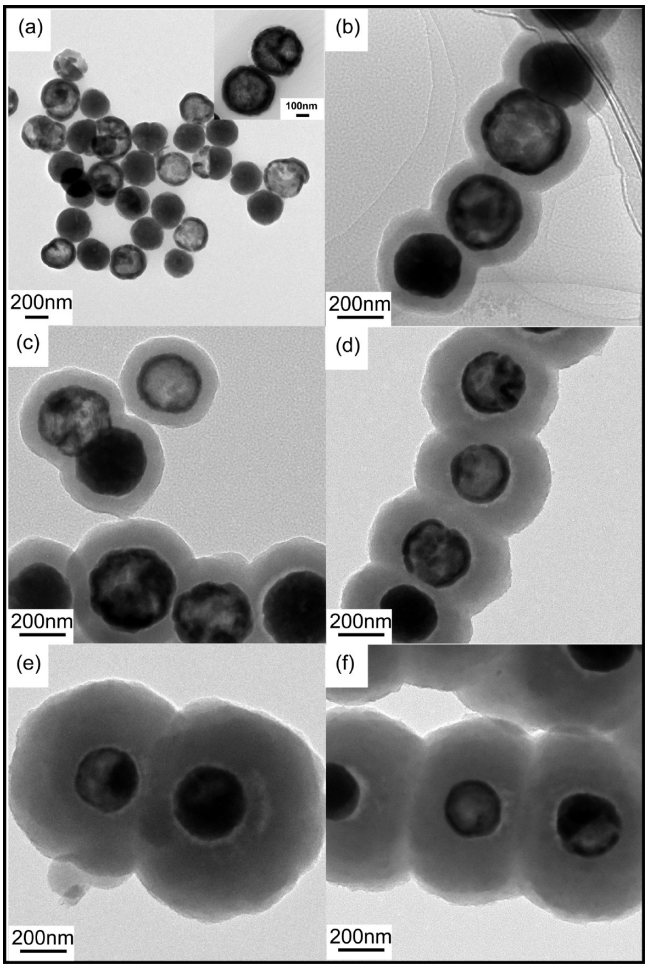

Figure 1. TEM images of (a) pure Fe_3O_4 microspheres and (b−f) Fe_3O_4−PEDOT core−shell microspheres prepared with different (EDOT)/(Fe_3O_4) ratios: (b) 10, (c) 15, (d) 20, (e) 30, and (f) 50.

To identify the components of the composites, especially the polymer composition, we performed FTIR analyses of Fe_3O_4, pure PEDOT, and Fe_3O_4−PEDOT composites prepared with (EDOT)/(Fe_3O_4) ratios of 10, 20, and 50. The spectra are shown in Figure 2. The FTIR spectrum of Fe_3O_4 (Figure 2A)

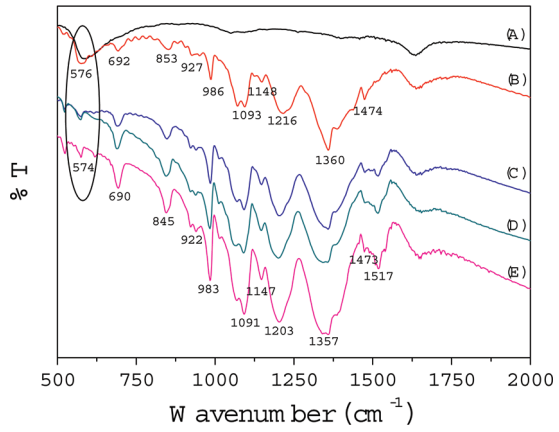

Figure 2. FTIR spectra of (A) Fe_3O_4; (B–E) Fe_3O_4–PEDOT composites prepared with different (EDOT)/(Fe_3O_4) ratios: (B) 10, (C) 20, (D) 50; and (E) pure PEDOT.

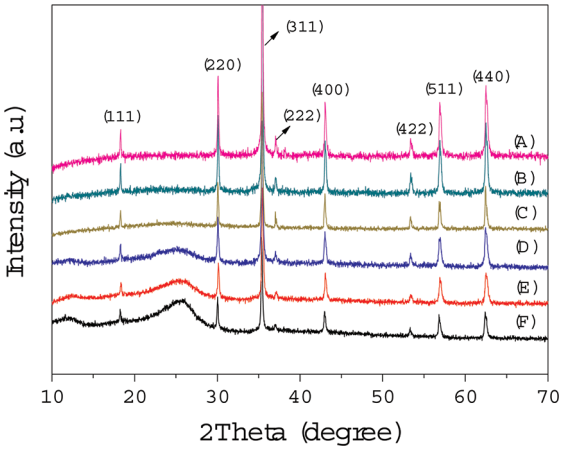

Figure 3. XRD patterns of (A) Fe_3O_4 microspheres and (B–F) Fe_3O_4–PEDOT composites prepared with different (EDOT)/(Fe_3O_4) ratios: (B) 10, (C) 15, (D) 20, (E) 30, and (F) 50.

shows characteristic peak at 588 cm^{-1}, attributed to the Fe–O bond stretching. This peak shifts to 576 cm^{-1} in the Fe_3O_4–PEDOT samples with a (EDOT)/(Fe_3O_4) ratio of 10 and continuously shifts to lower wavenumber and overlaps the peak of PEDOT with the increase of the (EDOT)/(Fe_3O_4) ratio. Figure 2E shows the spectra of pure PEDOT. The peaks at 690, 845, 922, and 983 cm^{-1} are attributed to the deformation modes of C–S–C in the thiophene ring; the peaks at 1091, 1147, and 1203 cm^{-1} are associated with the C–O–C bending vibration of the ethylenedioxy moiety; the peak at 1357 cm^{-1} is assigned to C–C stretching of the quinoidal structure; the peaks at 1473 and 1517 cm^{-1} are due to the C=C stretching of the quinoid structure of the thiophene ring. The main peaks of PEDOT shifts to high wavenumber with the increase of Fe_3O_4 in the composites compared to the pure PEDOT, which is due to some interaction of ferrite particles and polymer chains.[19] Above all, the FTIR spectra confirm the coexistence of Fe_3O_4 and PEDOT.

XRD patterns of Fe_3O_4 microspheres and Fe_3O_4–PEDOT composites prepared with different (EDOT)/(Fe_3O_4) ratios were also observed (Figure 3). Fe_3O_4 (Figure 3A) shows diffraction peaks at 2θ = 18.4, 30.1, 35.6, 37.2, 43.1, 53.5, 57.1, and 62.7°, which are in agreement with literatures.[18,20] These

Scheme 1. Formation Mechanism of Fe_3O_4–PEDOT Core–Shell Microspheres

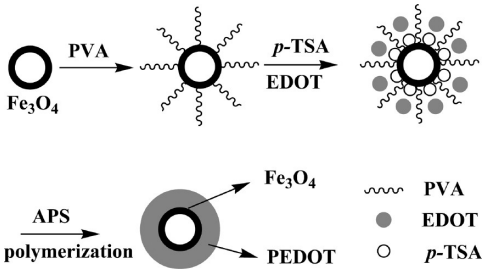

peaks correspond to the (111), (220), (311), (222), (400), (422), (511), and (440) lattice planes. When (EDOT)/(Fe_3O_4) ratios are 10 (Figure 3B) and 15 (Figure 3C), the diffraction peaks of Fe_3O_4–PEDOT composites are at the same position as the Fe_3O_4 microspheres (Figure 3A). However, with the (EDOT)/(Fe_3O_4) ratios increasing to 20 (Figure 3D) and 30 (Figure 3E), new peaks at 2θ = 25.6 and 11.7° appear. These two peaks become stronger with higher (EDOT)/(Fe_3O_4) ratios, accompanied with decreasing intensity of the Fe_3O_4 peaks. The peaks at 2θ = 25.6 and 11.7° prove the existence of PEDOT according to literature.[17] The diffraction patterns indicate that Fe_3O_4–PEDOT composites are composed of pure phase with no impurity.

Formation Mechanism. We explored the formation mechanism of the Fe_3O_4–PEDOT core–shell structure by a series of experiments. It was found that the Fe_3O_4–PEDOT core–shell structure could not form in the absence of PVA or *p*-TSA in the experiments. Without the inclusion of PVA, only a mixture of Fe_3O_4 microspheres and PEDOT was obtained. Most of PEDOT presented in amorphous state whereas a little polymer was found coated on the Fe_3O_4 microspheres to form a thin layer. There were Fe_3O_4 microspheres and a little polymer without *p*-TSA, and the polymer aggregated apart from the Fe_3O_4 microspheres. Overall, the coexistent of PVA and *p*-TSA is important during the formation of Fe_3O_4–PEDOT composites. In addition, we used Fe (*p*-toluene sulfonate) to replace APS and *p*-TSA in order to explore whether the oxidant with SO_3^- could act as the dual role of oxidant and dopant. The system did not form core–shell structure, which indicated that SO_3^- could not take the place of *p*-TSA. Then we suggest a possible mechanism of the Fe_3O_4–PEDOT core–shell microspheres formation shown in Scheme 1.

Fe_3O_4 particles are naturally hydrophilic due to plentiful hydroxyls on the particle surface.[21] The hydroxyl group in PVA can form hydrogen bonds with the hydroxyl group on Fe_3O_4 particles, which enables Fe_3O_4 particles to be well dispersed. Because of the weak static interactions between the SO_3^- group in *p*-TSA molecules and Fe_3O_4 particles,[14] *p*-TSA molecules can be absorbed on the surface of Fe_3O_4 particles. After EDOT monomer is added, the molecule tends to gather around the hydrophobic in PVA because of "similar compatibility". Subsequently, *p*-TSA serves as the dopant to enhance the protonation of EDOT, thus connects EDOT to the Fe_3O_4 particles. Once APS oxidant is introduced, the polymerization will occur and EDOT monomer will be nucleated on the surface of Fe_3O_4 microspheres. After EDOT nucleation occurring on the surface of Fe_3O_4 microspheres, the polymerization will continue to carry out with the as-formed PEDOT. During the formation, PVA as

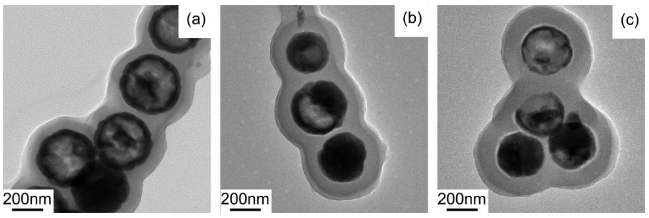

Figure 4. TEM images of Fe_3O_4−PEDOT composite ((EDOT)/(Fe_3O_4) = 10) with different polymerization time: (a) 24, (b) 48, and (c) 60 h.

Table 1. Electrical and Magnetic Properties of Fe_3O_4−PEDOT composites

composites with different (EDOT)/(Fe_3O_4)	conductivity (S cm^{-1})	M_s [a] (emu g^{-1})	M_r [b] (emu·g^{-1})	H_c [c] (Oe)
pure Fe_3O_4		84.8	7.6	61.9
10	5.28×10^{-4}	58.8	3.6	64.7
15	1.21×10^{-3}	40.3	2.2	58.8
20	1.06×10^{-2}	17	0.82	59.1
30	2.34×10^{-1}	11.3	0.56	61.1
50	3.13×10^{-1}	5.85	0.38	78.1

[a] Saturation magnetization. [b] Remnant magnetization. [c] Coercivity.

the stabilizer, promotes the "oriented attachment"[22] to join the as-formed PEDOT and gives rise to the shell. However, in the case of Fe (*p*-toluene sulfonate) replacing APS and *p*-TSA, the polymer shell did not form. This is because although the SO_3^- group in the Fe (*p*-toluene sulfonate) helped the attraction on the surface of Fe_3O_4 particles, it could not enhance the protonation of EDOT. That is to say, there is no link between Fe_3O_4 and EDOT, so the system could not form the core−shell structure.

To prove the mechanism further, the other stabilizer and dopants were used to prepare Fe_3O_4−PEDOT core−shell microspheres. It is found that polyvinyl pyrrolidone (PVP) as a typical stabilier can completely replace PVA. And *β*-naphthalenesulfonic acid (*β*-NSA) instead of *p*-TSA in Fe_3O_4−PEDOT formation can form core−shell structure too, though the core−shell structure was not as good as that using *p*-TSA as the dopant. The carbonyl group in PVP can form a hydrogen bond with the hydroxyl group on the surface of Fe_3O_4 particles. Thus PVP can stabilize the polymer sols, and improve the dispersion of the particles because of steric hindrance effecting from PVP adsorption on particle surface.[21] However, using oxalic acid as the dopant cannot produce Fe_3O_4−PEDOT core−shell microspheres. The results indicate the interaction between SO_3^- group and Fe_3O_4 microspheres plays an important role in the formation of Fe_3O_4−PEDOT core−shell structure. In summary, the stabilizer and sulfonic acid group together promote the formation of core−shell Fe_3O_4−PEDOT microsphere.

According to the suggested mechanism, EDOT monomer on the surface of Fe_3O_4 particles will increase and the organic layer will thicken as increase of the polymerization time. Figure 4 provides the evidence for this suppose. At a fixed (EDOT)/(Fe_3O_4) ratio of 10, the shell of Fe_3O_4−PEDOT microsphere increases from 60 to 100 nm following the reaction time increasing from 24 h (Figure 4a) to 48 h (Figure 4b). The shell increase becomes minor after a reaction time longer than 60 h (Figure 4c).

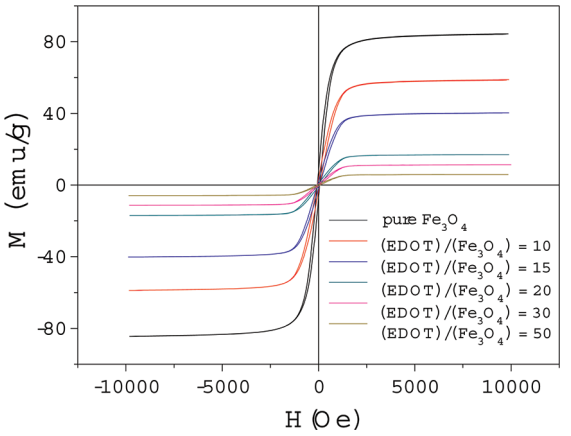

Figure 5. Magnetization curves applied magnetic field at room temperature of Fe_3O_4 microspheres and Fe_3O_4−PEDOT composites prepared with different (EDOT)/(Fe_3O_4) ratios.

Electric and Magnetic Properties. The electrical properties of the obtained Fe_3O_4−PEDOT composites were measured by four-point probe method and the conductivities are displayed in Table 1. It is found that the conductivities of the composites at room temperature are in the range of 1×10^{-4} to 1×10^{-1} S cm^{-1} and increase with the (EDOT)/(Fe_3O_4) ratio increasing. The tendency is consistent with the shell thickness (Figure 1b−f) because the conductivity is mainly determined by the polymer. The thicker the shell is, the higher the conductivity is.

The magnetic properties of Fe_3O_4 and Fe_3O_4−PEDOT microspheres prepared with different (EDOT)/(Fe_3O_4) ratios were investigated with a VSM which features a sensitivity of 1×10^{-5} emu. And Figure 5 shows the hysteresis loops of the obtained samples in the applied magnetic field sweeping from −10 to 10 kOe at room temperature. The magnetic parameters corresponding to Figure 5 are shown in Table 1. The pure Fe_3O_4 is a typical superparamagnetic material, presenting high saturation magnetization (M_s), high remnant magnetization (M_r), and low coercivity (H_c). With the increase of the (EDOT)/(Fe_3O_4) ratio, the saturation magnetization and remnant magnetization are decreased, due to the decrease of Fe_3O_4 content in the composites. The independence of coercivity on the (EDOT)/(Fe_3O_4) ratio suggests that the superparamagnetism has the same origin, from Fe_3O_4. It is clear from Table 1 that the Fe_3O_4−PEDOT composites exhibit good magnetic properties and low conductivities with lower (EDOT)/(Fe_3O_4) ratios, while low magnetic properties and high conductivities with higher (EDOT)/(Fe_3O_4) ratios.

Microwave Absorbing Properties. For a microwave-absorbing layer terminated by a short circuit, the normalized input impedance is related to the impedance in free space, Z_{in}, and reflection loss (RL) is related to the normal incident plane wave, which can be given by the theory of the absorbing wall.[23]

$$Z_{in} = \sqrt{\frac{\mu_r}{\varepsilon_r}} \tanh\left[j \frac{2\pi}{c} \sqrt{\mu_r \varepsilon_r} f d \right] \quad (1)$$

$$RL\ (\mathrm{dB}) = 20 \log \left| \frac{Z_{in} - 1}{Z_{in} + 1} \right| \quad (2)$$

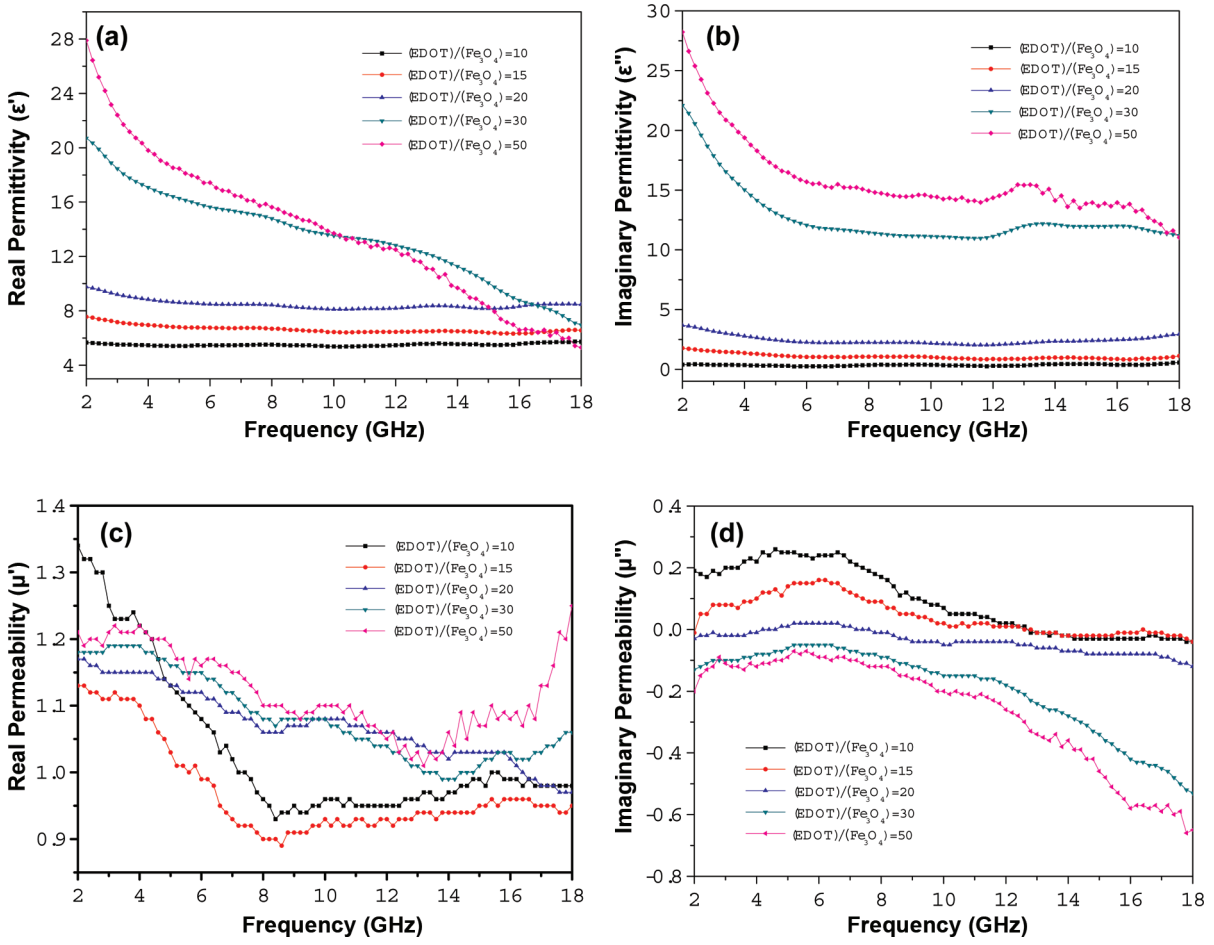

Figure 6. Electromagnetic parameters of Fe_3O_4—PEDOT composites with different (EDOT)/(Fe_3O_4) ratios at 50% volume fraction in the 2—18 GHz range: (a) real and (b) imaginary parts of the relative complex permittivity; (c) real and (d) imaginary parts of the relative complex permeability.

where c is the velocity of light in free space, f is the frequency, and d is the layer thickness. The relative complex permittivity (ε_r) and relative permeability (μ_r) of the absorbing medium are expressed as $\varepsilon_r = \varepsilon' - j\varepsilon''$, $\mu_r = \mu' - j\mu''$. The impedance matching condition is determined by the combination of the six parameters: ε', ε'', μ', μ'', f, and d.

The real permittivity (ε') and real permeability (μ') symbolize the storage ability of electromagnetic energy,[24] while the imaginary permittivity (ε'') is related to the dissipation of energy and the magnetic loss is expressed by imaginary permeability (μ'').[19]The curve of ε', ε'', μ', and μ'' of Fe_3O_4—PEDOT composites with different (EDOT)/(Fe_3O_4) ratios at 50% volume fraction are shown as Figure 6. It is observed that the samples with higher (EDOT)/(Fe_3O_4) ratios show higher values of ε' and ε'' (Figure 6a,b), which is related to higher conductivities. Moreover, the μ' values obviously decrease and then increase with the frequency increasing in the 2—18 GHz range (Figure 6c). When (EDOT)/(Fe_3O_4) ratios are 10 and 15, the μ'' values exhibit positive in the whole range; while a negative μ'' value means the magnetic energy is radiated out with no absorption.[24] That is to say, the composites mainly exhibit electrical losses when (EDOT)/(Fe_3O_4) ratios are 20, 30, and 50.

On the basis of formulas 1 and 2, we calculated the RL of Fe_3O_4—PEDOT composites with different (EDOT)/(Fe_3O_4) ratios in the frequency range of 2—18 GHz at 50% volume fraction. Figure 7 shows the RL variation when the layer thickness is 2 mm. With a (EDOT)/(Fe_3O_4) ratio of 20, the minimum RL of the composite is −27.6 dB, which is better than pure PEDOT in our research before (−24 dB).[16] The minimum

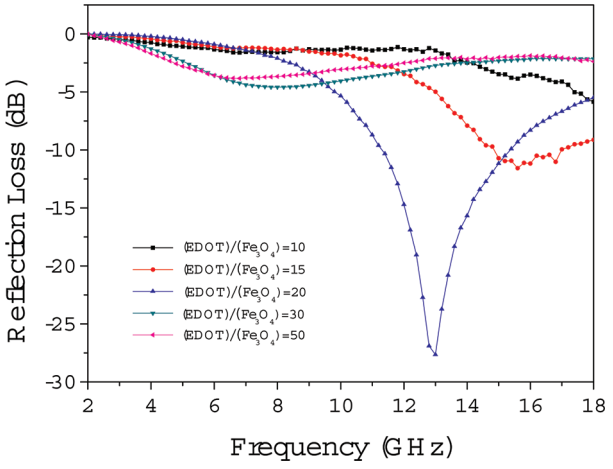

Figure 7. Reflection losses in the thickness of 2 mm of the Fe_3O_4—PEDOT composites prepared with different (EDOT)/(Fe_3O_4) ratios at 50% volume fraction.

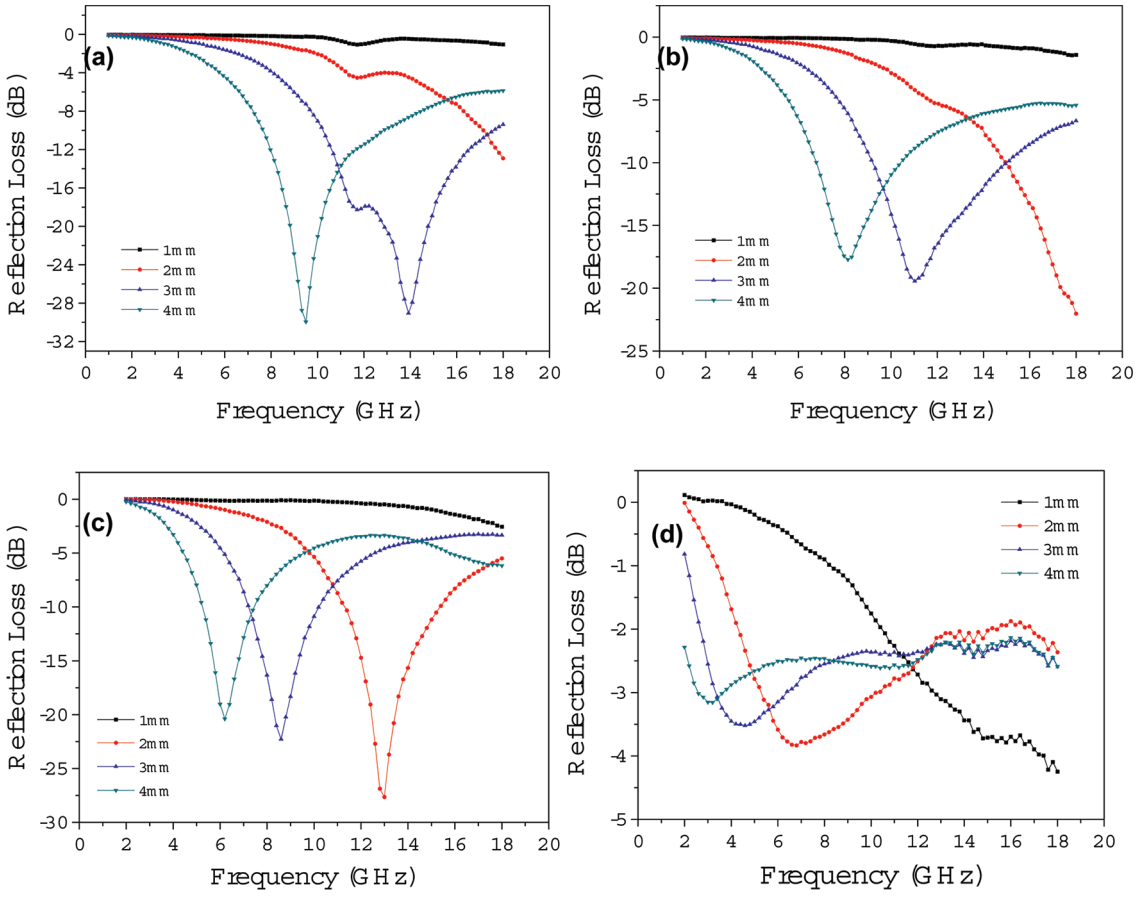

Figure 8. Reflection losses in different thickness of Fe_3O_4—PEDOT composites with (a) (EDOT)/(Fe_3O_4) = 20 and (b) 50 at 20% volume fraction (c) (EDOT)/(Fe_3O_4) = 20 and (d) 50 at 50% volume fraction.

reflection losses of the specimen with the (EDOT)/(Fe_3O_4) = 30 and 50 are −4.6 dB and −3.8 dB, respectively. Comparing with the conductivities in Table 1, it can be found that the composites with higher conductivities at (EDOT)/(Fe_3O_4) = 30 and 50 do not correspond to better absorbing parameters. This indicates that both higher conductivity and lower conductivity ((EDOT)/(Fe_3O_4) = 10) are not beneficial to improving microwave absorbing and the maximum microwave absorbing corresponds to an intermediate conductivity.[25,26]

In addition, to study the influence of volume fraction on microwave absorbing property, the electromagnetic parameters of Fe_3O_4—PEDOT composites with (EDOT)/(Fe_3O_4) = 20 and 50 at 20% volume fraction were measured and the calculated reflection losses are shown as panels a and b in Figure 8, respectively. Meanwhile, panels c and d in Figure 8 show the calculated reflection losses of Fe_3O_4—PEDOT composites with (EDOT)/(Fe_3O_4) = 20 and 50 at 50% volume fraction, respectively. When the volume fraction is 20% (Figure 8a), the sample with (EDOT)/(Fe_3O_4) = 20 exhibits excellent microwave absorbing property in the layer thickness range of 3- 4 mm and the minimum RL is −30 dB at 9.5 GHz with a layer thickness of 4 mm; when the volume fraction is 50% (Figure 8c), this composite exhibits good microwave absorbing property in the layer thickness range of 2−4 mm and the minimum RL is −27.6 dB at 13 GHz with a layer thickness of 2 mm. Besides, the RL of the Fe_3O_4—PEDOT composite with (EDOT)/(Fe_3O_4) = 50 at 20% volume fraction (Figure 8b) is larger than the sample at 50% volume fraction (Figure 8d) and the minimum RL is −22 dB at 18 GHz with a layer thickness of 2 mm. The result indicates that the conductivity, volume fraction and layer thickness all have great impacts on microwave absorbing property.

CONCLUSIONS

Uniform core−shell Fe_3O_4—PEDOT microspheres were successfully synthesized by a two-step method. The selection of both stabilizer and dopant are essential for the formation of the composites. The properties of the composites are significantly influenced by the (EDOT)/(Fe_3O_4) ratio. The Fe_3O_4—PEDOT composites exhibited good conductivities at high (EDOT)/(Fe_3O_4) ratios and excellent magnetic properties at low (EDOT)/(Fe_3O_4) ratios. The reflection losses calculated by the theory of the absorbing wall showed that the Fe_3O_4—PEDOT composite with (EDOT)/(Fe_3O_4) = 20 exhibited the best microwave absorbing property in the range of 2−18 GHz. The minimum RL reached approximated −30 dB at the thickness of 4 mm. In summary, the two-step synthesis and electromagnetic core−shell Fe_3O_4—PEDOT composites will have a promising application in microwave absorbing field.

AUTHOR INFORMATION

Corresponding Author

*E-mail: huxiujie@mail.ipc.ac.cn (X.H.); zhou_shuyun@mail.ipc.ac.cn (S.Z.). Fax: +86 010-82543517; Tel: +86 010-82543515.

■ ACKNOWLEDGMENT

This work was supported by National Natural Science Foundation of China (20874112 and 60808022). The authors thank X. Huang and M. Wang for the assistance in TEM characterization.

■ REFERENCES

(1) Kawaguchi, H. *Prog. Polym. Sci.* **2000**, *25*, 1171–1210.
(2) Zhang, L.; Wan, M. *J. Phys. Chem. B* **2003**, *107*, 6748–6753.
(3) Kurlyandskaya, G. V.; Cunanan, J.; Bhagat, S. M.; Aphesteguy, J. C.; Jacobo, S. E. *J. Phys. Chem. Solids* **2007**, *68*, 1527–1532.
(4) Marchessault, R. H.; Rioux, P.; Raymond, L. *Polymer* **1992**, *33*, 4024–4028.
(5) Lu, W.; Shen, Y.; Xie, A.; Zhang, W. *J. Magn. Magn. Mater.* **2010**, *322*, 1828–1833.
(6) Hu, F. Q.; Wei, L.; Zhou, Z.; Ran, Y. L.; Li, Z.; Gao, M. Y. *Adv. Mater.* **2006**, *18*, 2553–2556.
(7) Seino, S.; Kinoshita, T.; Otome, Y.; Nakagawa, T.; Okitsu, K.; Nakayama, T.; Sekino, T.; Niihara, K.; Yamamoto, T. A. *J. Ceram. Process. Res.* **2004**, *5*, 136–139.
(8) Rana, S.; White, P.; Bradley, M. *Tetrahedron Lett.* **1999**, *40*, 8137–8140.
(9) Kuramitz, H. *Anal. Bioanal. Chem.* **2009**, *394*, 61–69.
(10) Yang, X.; Zhang, X.; Ma, Y.; Huang, Y.; Wang, Y.; Chen, Y. *J. Mater. Chem.* **2009**, *19*, 2710–2714.
(11) Ni, S.; Wang, X.; Zhou, G.; Yang, F.; Wang, J.; He, D. *J. Alloys Compd.* **2010**, *489*, 252–256.
(12) Liu, J.; Wan, M. *J. Polym. Sci., Part A: Polym. Chem.* **2000**, *38*, 2734–2739.
(13) Deng, J.; Peng, Y.; He, C.; Long, X.; Li, P.; Chan, A. S. C. *Polym. Int.* **2003**, *52*, 1182–1187.
(14) Lu, X.; Mao, H.; Zhang, W. *Polym. Compos.* **2009**, *30*, 847–854.
(15) Reddy, K. R.; Lee, K. P.; Gopalan, A. I. *Colloids. Surf., A* **2008**, *320*, 49–56.
(16) Ni, X.; Hu, X.; Zhou, S.; Sun, C.; Bai, X.; Chen, P. *Polym. Adv. Technol.* **2011**, *22*, 532–537.
(17) Reddy, K. R.; Park, W.; Sin, B. C.; Noh, J.; Lee, Y. *J. Colloid Interface Sci.* **2009**, *335*, 34–39.
(18) Lv, Q. R.; Fang, Q. Q.; Liu, Y. M.; Wang, W. N. *Chin. J. Phys.* **2010**, *48*, 417–423.
(19) Ohlan, A.; Singh, K.; Chandra, A.; Dhawan, S. K. *ACS Appl. Mat. Interfaces* **2010**, *2*, 927–933.
(20) Hu, P.; Yu, L.; Zuo, A.; Guo, C.; Yuan, F. *J. Phys. Chem. C* **2008**, *113*, 900–906.
(21) Guo, L.; Pei, G.-L.; Wang, T.-J.; Wang, Z.-W.; Jin, Y. *Colloids Surf., A* **2007**, *293*, 58–62.
(22) Yang, Q.; Tang, K.; Wang, C.; Qian, Y.; Zhang, S. *J. Phys. Chem. B* **2002**, *106*, 9227–9230.
(23) Abbas, S. M.; Dixit, A. K.; Chatterjee, R.; Goel, T. C. *Mater. Sci. Eng., B* **2005**, *123*, 167–171.
(24) Wang, C.; Han, X.; Xu, P.; Wang, J.; Du, Y.; Wang, X.; Qin, W.; Zhang, T. *J. Phys. Chem. C* **2010**, *114*, 3196–3203.
(25) Xu, P.; Han, X.; Wang, C.; Zhao, H.; Wang, J.; Wang, X.; Zhang, B. *J. Phys. Chem. B* **2008**, *112*, 2775–2781.
(26) Unsworth, J.; Kaynak, A.; Lunn, B.; Beard, G. *J. Mater. Sci.* **1993**, *28*, 3307–3312.